Journal of the European Ceramic Society 22 (2002) 1217–1223

www.elsevier.com/locate/jeurceramsoc

Development of anisotropic microstructure in uniaxially pressed alumina compacts

Anze Shui*, Midori Saito, Nozomu Uchida, Keizo Uematsu

Department of Chemistry, Nagaoka University of Technology, Kamitomioka, Nagaoka, Niigata 940-2188, Japan

Received 25 May 2001; received in revised form 3 August 2001; accepted 5 August 2001

Abstract

Alumina compacts are prepared by uniaxial pressing followed by cold isostatic pressing (CIP). Anisotropic microstructures of the compacts and their sintered bodies are reported. Anisotropic grain growth with sintering time was systematically examined through direct measurement of grain dimensions on SEM micrographs in various conditions. Experimental results indicated that average grain size was always larger in the plane parallel to the direction of uniaxial pressing, than in its perpendicular plane, for all sintering conditions. The difference in the average grain size increased in these planes with sintering time. The grain growth followed the cubic law and the rate constants were 4.8×10^{-21} and $1.9\times10^{-21}(m^3/s)$, for the former and the latter, respectively, in specimen uniaxial pressed at 100 MPa and CIPed at 100 MPa. Many intra-granule fractures were observed in the compact in the plane perpendicular the pressing direction comparing with its parallel plane.

Keywords: Al_2O_3; Anisotropy; Grain growth; Pressing; Sintering

1. Introduction

Two recent papers reported an anisotropic packing structure of powder particles in uniaxially pressed alumina compact made of industrial low soda alumina.[1,2] The particles, which characteristically have elongated shapes, are aligned with their long axis perpendicular to the pressing direction. One of the significant consequences of the alignment was the deformation of compact during sintering. The shrinkage in sintering was always larger in the height direction of the compact (i.e. the direction parallel to the uniaxial pressing direction, described as H direction hereafter) than the diametical direction (i.e. the direction perpendicular to the pressing direction, described as D direction hereafter). Where, H plane is defined as the plane parallel the pressing direction, and D plane as its perpendicular plane. This anisotropic particle packing may also develop an anisotropic microstructure in the H and D planes in sintered ceramics. However, there are only few studies on this subject except in the systems with significantly anisometric particles, such as clay base materials. It is interesting to clarify the effect of the pressing direction on the microstructure development for uniaxially pressed alumina compacts.

In systems of fine ceramics, anisotropic grain growth has been reported in systems of hot pressing and tape casting.[3–6] The particle orientation developed markedly an anisotropic microstructure and thus mechanical properties. The bending strength and fracture toughness changed with the plane of specimen. However, the rate of anisotropic grain growth was not quantitatively shown in those studies. No systematic study has been reported on the system involving uniaxial pressing, in which the driving force for particle orientation is very small.

In this study, the development of anisotropic microstructures is systematically examined on uniaxially pressed alumina compacts, and the rate of anisotropic grain growth is quantitatively shown. Changes of sintering shrinkage and sintered density with sintering time and temperature are also examined.

2. Experiment

A commercial powder was used in this study, 160SG-1, Showadenko, Japan. The nominal average particle size is 0.4 μm, and the average aspect ratio is 1.6 as determined on SEM micrographs in a separate study.[2]

* Corresponding author. Tel.: +81-258-47-9337; fax: +81-258-47-9300.

E-mail address: zei@stn.nagaokaut.ac.jp (A. Shui).

0955-2219/02/$ - see front matter
PII: S0955-2219(01)00434-4

Slurry containing 50 mass% alumina powder was prepared by mixing it with distilled water and 2 mass% PVA (PVA105, Kuraray, Japan) in a ball mill. Spray dried alumina granules were prepared from the slurry with a spray drier (Model SD13, Mitsui Kozan, Japan, inner diameter 1.3 m) with the inlet and outlet air temperatures, 200 and 100 °C, respectively. Compacts (diameter 15 mm×height 5–6 mm) were prepared in metal die at pressing 0–100 MPa and subsequent CIP at 100–200 MPa. The compacts were sintered in an electric furnace at 1100–1600 °C in air with heating rate 10 °C/min and holding time 2–24 h. The shrinkage of the compact during sintering was determined from its dimensional change in sintering. The relative density of the green compact was measured with a mercury porosimetry (Pore Sizer 9320, Shimadzu, Japan). The relative density of sintered body was determined with the Archimedean method using distilled water. For the SEM observation, specimens (4×4 mm) were cut from the centers of compacts and sintered bodies, the H plane (parallel the pressing direction) and D Plane (perpendicular the pressing direction) were examined, respectively. The planes of sintered specimen were finished with diamond slurry (0.5 μm), and thermally etched at 1550 °C for 30 min in air. Before the SEM observation, all specimens were treated with gold sputtering. The particle and grain sizes were directly measured as diameters of their equivalent area circles from the SEM micrographs for over 900 particles and grains at various conditions. The magnification of the microscope was calibrated with a standard sample of known particle size.

3. Results

Fig. 1 are SEM micrographs of fracture surfaces for the compact (uniaxial pressing 40 MPa, CIP 100 MPa) in the H and D planes. The structure is clearly different in the two planes. In side-view (H plane-view), the granules originally having spherical shape, deformed into elliptical shape in the H plane. But in top-view (D plane-view), they retained nearly spherical shape in the D plane. The similar anisotropic deformation of the granules was also noted in the observation with the immersion liquid method, a characterization tool developed in our research group.[1,2,7,8] The fracture behavior was clearly different for the two planes; the intra-granule fracture was more significant in the D plane than the H plane.

Fig. 2 shows SEM micrographs of fracture surfaces of the compact (uniaxial pressing 100 MPa, CIP 100 MPa) at high magnification in the H and D planes. The particle size was analyzed to examine a difference of particle packing microstructure in the H and D planes. In the analysis, the particle size was determined on about 1000 particles and was found to be slightly smaller in the D plane (0.36±0.01μm) than the H plane (0.39±0.01μm).

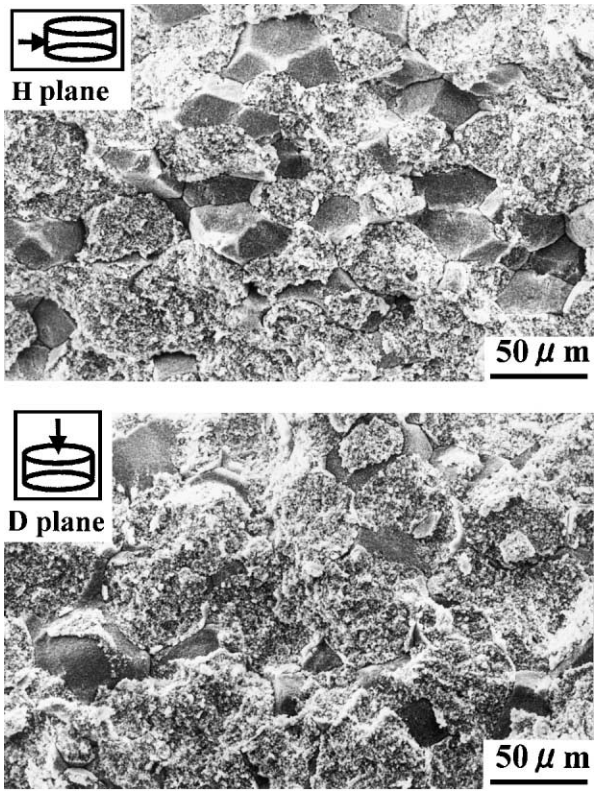

Fig. 1. SEM micrographs of fracture surfaces for the compact (uniaxial pressing at 40 MPa, CIP at 100 MPa) in H and D planes.

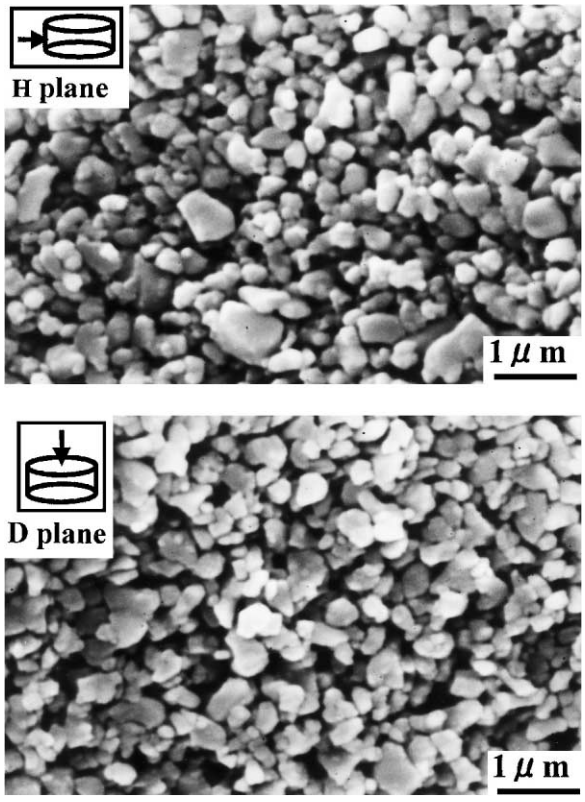

Fig. 2. SEM micrographs of fracture surfaces of the compact (uniaxial pressing at 100 MPa, CIP at 100 MPa) at high magnification in H and D planes.

This indicates that the particle packing structure is different in the two planes.

Fig. 3 shows the change of sintering shrinkage for the co MPact (uniaxial pressing at 100 MPa, CIP at 200 MPa) with sintering temperature for holding time 2 h. Anisotropic shrinkage was again noted during sintering similar to our previous papers.[1,2] The sintering shrinkage was almost the same in the H direction (height direction) and D direction (diametric direction) for sintering under about 1200 °C, but was always larger in the H direction than the D direction at higher temperatures. The difference of shrinkage for the two directions increased as the sintering temperature increased. Repeated measurements showed the same results. The error in the measurement is about a line width in the figure.

Fig. 4 shows change of sintered density of the co MPact (uniaxial pressing 100 MPa, CIP 200 MPa) with sintering temperature for holding time 2 h. The sintered density increased with increasing temperature. The results are divided into three stages. The initial densification stage is about until 1200 °C, where the rate of the densification is low. The middle densification stage is about from 1200 to 1500 °C, where the rate is high. The final stage is noted at temperature exceeding 1500 °C, where the rate becomes low again.

Fig. 5 shows changes of sintering shrinkage with sintering time for various compacts (uniaxial pressing at 100 MPa, and CIP at 0, 100 or 200 MPa) at 1600 °C. Data are marked with the CIP pressure and the measurement direction; e.g., 200 MPa-H means the co MPact CIPed at 200 MPa and measured in the H direction. The shrinkage was the highest at the sintering time 2 h for all specimens, and decreased with increasing sintering time. The shrinkage was always higher in the H direction than the D direction, and the difference of shrinkage in the two directions decreased as the sintering time increased.

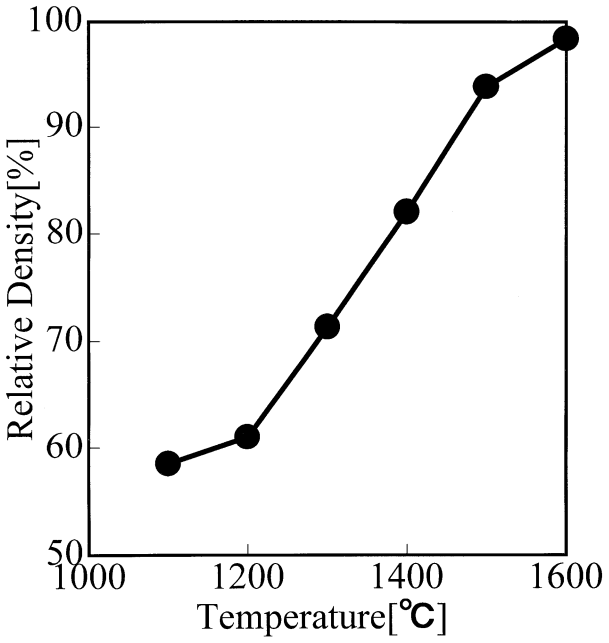

Fig. 4. Change of sintered density of the compact (uniaxial pressing at 100 MPa, CIP at 200 MPa) with sintering temperature for holding time 2 h.

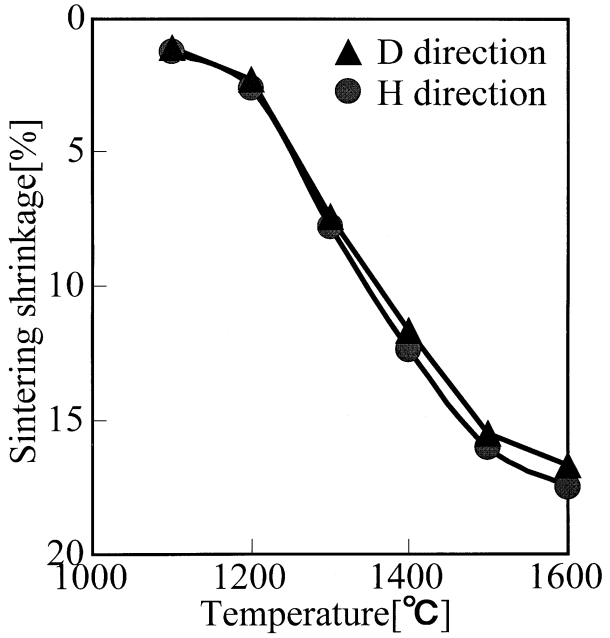

Fig. 3. Change of sintering shrinkage for the compact (uniaxial pressing at at 100 MPa, CIP at at 200 MPa) with sintering temperature for holding time 2 h.

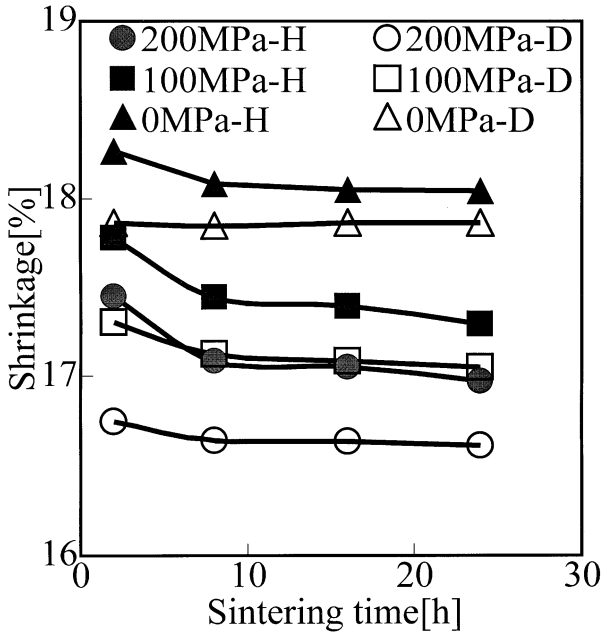

Fig. 5. Changes of sintering shrinkage with sintering time for various compacts (uniaxial pressing at 100 MPa, and CIP at 0, 100 or 200 MPa) at 1600 °C.

Fig. 6 shows changes of sintered density with sintering time for various compacts (uniaxial pressing at 100 MPa, and CIP at 0, 100 or 200 MPa) at 1600 °C. The sintered density was the highest in sintering time 2 h for all compacts. It decreased with increasing sintering time for these compacts.

Fig. 7 shows SEM micrographs of sintered body (uniaxial pressing at 100 MPa, and CIP at 100 MPa) in the H and D planes at 1600 °C for 24 h. There is a clear difference in the microstructure. The grain size was more uniform in the H plane than the D plane. Small grains were more dominant in the D plane than the H plane. The size of large grains also appears in this plane. Clearly, the grain growth is more non-uniform in the D plane. The similar anisotropic microstructure was observed in the two planes on other sintered body, which was uniaxially pressed at 100 MPa and CIPed at 200 MPa. However, there is no clear tendency to suggest the particle orientation in these SEM micrographs, such as alignment of long grains. In past research, we also tried repeatedly to characterize the particle orientation in those compacts with X-ray diffraction analysis including the Rocking curve for many times.[9,10] We could not detect it either in this method.

Fig. 8 shows grain size distributions in sintered body (uniaxial pressing at 100 MPa, and CIP at 100 MPa) at 1600 °C for 24 h in the H and D planes. The grain size ranged from about 2 to about 32 μm in both planes. There was a difference of grain size distribution in these planes. The average grain size is defined as arithmetic mean of all grains in various conditions. The average grain size was smaller in the D plane; 7.2±0.1μm and 4.9±0.1 μm in the H plane and D plane, respectively. The average grain size differed about 47% in two planes.

Fig. 9 shows the grain size distributions in sintered body (uniaxial pressing at 100 MPa, and CIP at 200 MPa) at 1600 °C for 24 h in the two planes. The grain size ranged from about 2 to about 40 μm in these planes. The average grain size was again smaller in the D plane; 11.2±0.1 and 7.6±0.1 μm in the H and D planes, respectively. Interestingly, the average grain size also differed about 47% in the two planes, too.

Fig. 10(a) shows changes of the average grain size with sintering time for the compact (uniaxial pressing 100 MPa, and CIP at 100 MPa) in the H and D planes. The grain size increased with increasing sintering time in both planes. The grain size was always larger in the H plane than the D plane. The difference of grain size for the two planes increased as the sintering time increased.

The rate constant of grain growth can be determined for the two planes, with the assumption that the grain growth follows the next equation,

$$G^3 - G_0^3 = kt \tag{1}$$

Where the G_0 and G are grain diameters at the sintering time zero and t, respectively, and k is the rate constant of the grain growth.

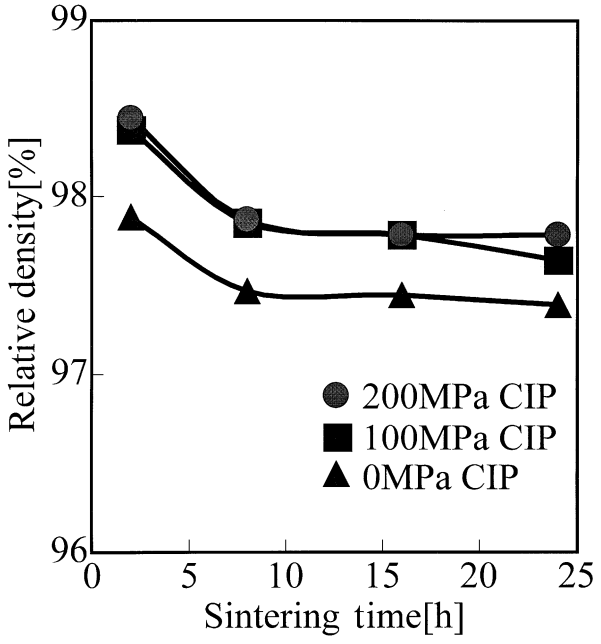

Fig. 6. Changes of sintered density with sintering time for various compacts (uniaxial pressing at 100 MPa, and CIP at 0, 100 or 200 MPa) at 1600 °C.

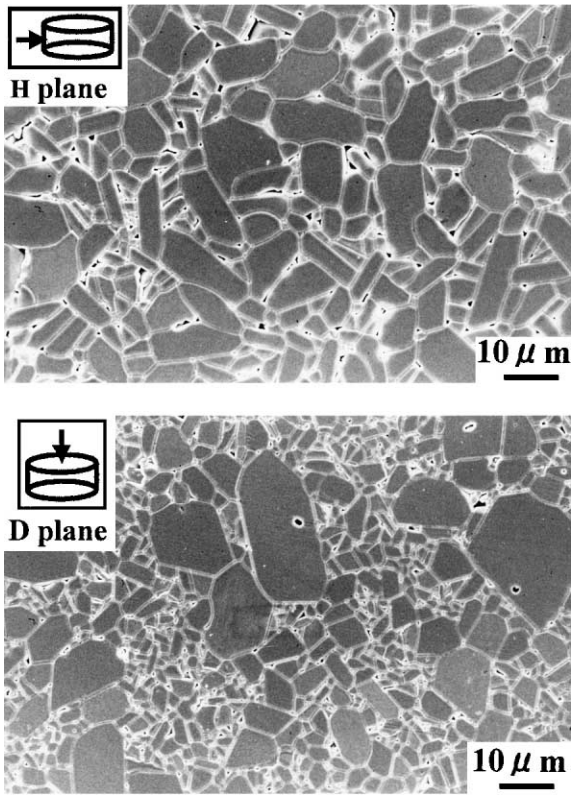

Fig. 7. SEM micrographs of sintered body (uniaxial pressing at 100 MPa, and CIP at 100 MPa) in H and D planes at 1600 °C for 24 h.

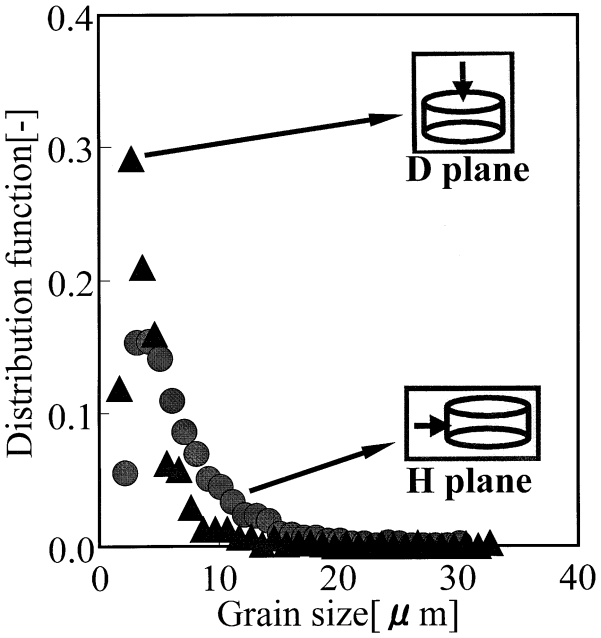

Fig. 8. Grain size distributions in sintered body (uniaxial pressing at 100 MPa, and CIP at 100 MPa) at 1600 °C for 24 h in the two planes.

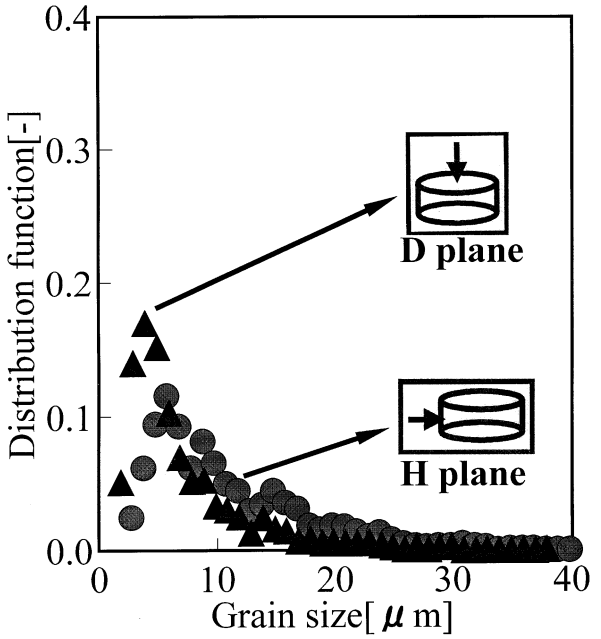

Fig. 9. Grain size distributions in sintered body (uniaxial pressing at 100 MPa, and CIP at 200 MPa) at 1600 °C for 24 h in the two planes.

Fig. 10(b) shows values of the rate constant k calculated from the data in Fig. 10(a) for the two planes. The constants were 4.8×10^{-21} and $1.9\times10^{-21}(m^3/s)$ in the H plane and D plane, respectively. These values are in reasonable agreement with past results. Bae et al. showed that value of the K was $7.5\times10^{-21}(m^3/s)$ at 1600 °C for high purity alumina (>99.999%).[11,12] The small difference among the studies is understandable. In the present study, the purity of alumina powder was 99.8%, with MgO 500 ppm from the manufacturer.

The value of the constant k differed about a factor of two in the two planes. Clearly, the grain growth of the uniaxially pressed compact considerable varies with direction. The grain growth rate is significantly larger in the H plane than the D plane.

4. Discussions

The results of this study again showed a clear difference of structure with plane in the compacts made by uniaxial pressing. This anisotropic structure of the compact resulted in anisotropic shrinkage in sintering and developed an anisotropic microstructure. The anisotropic structure was preserved in the compact even after CIP.

Fig. 1 clearly showed that structure differed in the H and D planes in the compact. These micrographs provided a proof, which anisotropic microstructure existed in the uniaxially pressed compacts. The apparent particle size was slightly larger in the H plane than D plane in Fig. 2. These results can be explained by anisotropy of the particle orientation reported in our previous papers on the similar system.[1,2] In these studies, the orientation was examined with a polarized light microscope with the immersion liquid method.

The results of Figs. 3 and 5 clearly showed the anisotropic shrinkage of the compacts in sintering. It should be noticed that the anisotropic shrinkage occurs during sintering for all sintering temperature and time in the uniaxially pressed compacts even after CIP at a high pressure (200 MPa). The largest difference in the shrinkage in the H (height) and D (diametric) directions is 0.8%, which was noted at uniaxial pressing 100 MPa and CIP 200 MPa at 1600 °C for 2 h. This result directly shows that CIP can not reduce the anisotropy, i.e., anisotropic particle orientation produced by uniaxial pressing, and continues in the compact even after CIP treatment at a high pressure.

The particle packing density is considerably uniform in the compacts from their results of the 3D X-ray tomography, which will be shown in a separate paper. The error of the sintering shrinkage for various compacts is less than 0.1%.

The anisotropic particle packing causes not only the anisotropic sintering shrinkage, but also the significant anisotropy in grain growth rate and microstructure in sintered bodies as noted in Figs. 7–10. Origin of the anisotropic grain growth is again ascribed to anisotropy of the particle orientation developed by the shear stress during uniaxial pressing, which depends on the particle shape of the raw material. The average aspect ratio of

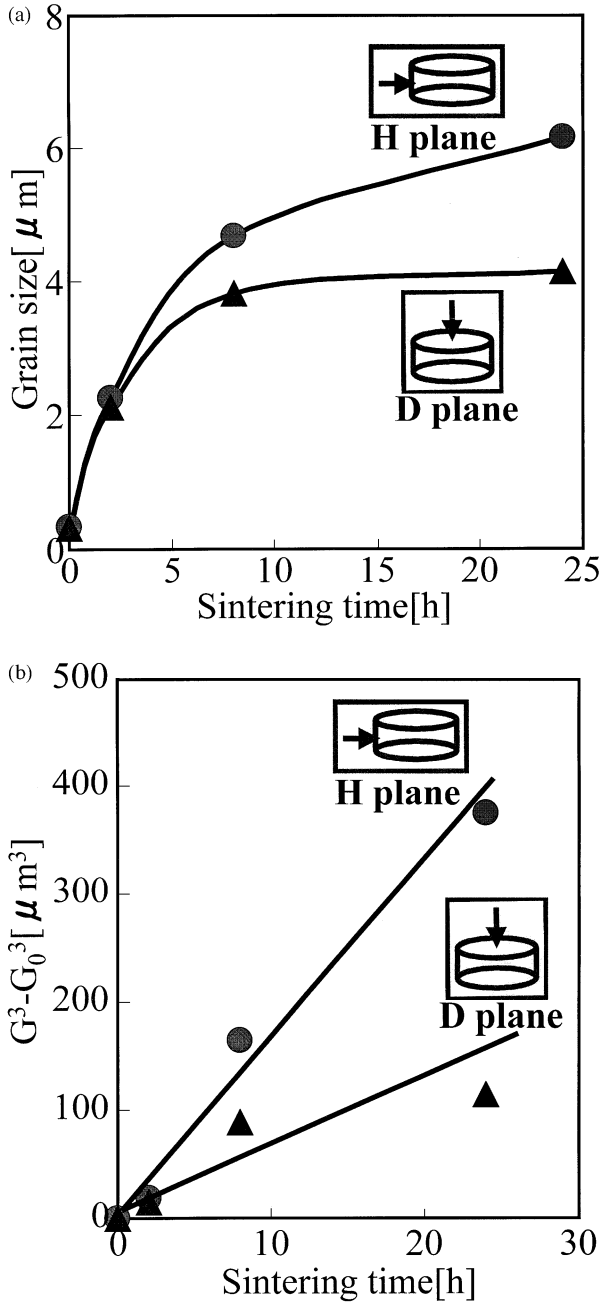

Fig. 10. (a). Changes of average grain size with sintering time for the compact (uniaxial pressing at 100 MPa, and CIP at 100 MPa) in the two planes. (b) Values of the rate constant K of grain growth for the compact in the two planes.

the raw alumina particles is about 1.6 from our previous study.[2] The raw material is a general industrial powder used widely in ceramics production. Accordingly, this study can be expected to have a wide reference value in industrial production and research fields.

There are many researches about abnormal (or anisotropic) grain growth of additive or seeded systems.[13–17] However, origin of the anisotropic grain growth was additive or seed in these studies. It is different at all to the origin in this study.

The significant difference of microstructures (Fig. 7) can be explained from the growth behavior of alumina. In a system containing seeds of alumina single crystallites, it is well known that the grain growth is larger in c-plane. In this study, the longest axis of the alumina particle corresponds the a-axis. The particles are weakly aligned in the H plane (parallel the pressing direction) with their a-axis perpendicular the pressing direction, and randomly aligned in the D plane (perpendicular the pressing direction). Consequently, the apparent grain size was more non-uniform in the D plane than the H plane. Surfaces of the larger grains viewed directly in Fig. 7(b) correspond to the c-plane of the alumina particles. Because the c-plan growth is larger during sintering, they appear large.

The decrease of density with long sintering time in Fig. 6 has been documented in a standard textbook. Kingery et al. explained this phenomenon by the growth of pore volume with the grain growth, i.e. bloating or blistering.[18] In this process, the gases are pressurized in pores to resist the interfacial force for shrinking. The growth of pore by coalescence reduces the pressure needed for equilibrium and thus increases the total pore volume, since the pressure in the pore decreases with increasing pore size.

It is necessary to comment on the method used for determining the sizes of particles and grains in this study. The size was directly measured as a diameter of the equivalent area circle on at least 900 particles and grains in various conditions from their SEM micrographs. This number is much larger than 200–300 commonly determined with the intercept method[19] in many researches on grain growth. The average size 0.39 ± 0.01 μm agreed well to the value 0.4 μm provided by the manufacturer in Fig. 2(a).

In addition, anisotropies of mechanical properties of the sintered bodies such as bending strength and fracture toughness have not been examined in this study. Hot pressing and tape casting systems showed the anisotropic mechanical properties.[3–6,20] The similar results may be expected from the anisotropic microstructure of the sintered body in this study.

5. Conclusions

Anisotropic microstructures in uniaxially pressed alumina compacts and sintered bodies have been systematically and quantitatively studied. The rate of grain growth was above two times larger in the plane parallel the pressing direction than its perpendicular plane in the compacts made at uniaxial and CIP pressures 100 MPa. The origin is attributed to anisotropy of the particle orientation developed during the uniaxial pressing.

Acknowledgements

The study was supported by the ministry of education, culture, science, sports and technology.

References

1. Shui, A., Zhang, Y., Uchida, N. and Uematsu, K., Origin of shape deformation during sintering alumina compacts. *J. Ceram. Soc. Japan*, 1998, **106**, 873–876.
2. Shui, A., Kato, Z., Tanaka, S., Uchida, N. and Uematsu, K. Sintering deformation caused by particle orientation in uniaxially and isostatically pressed alumina compacts. *J. Eur. Ceram. Soc.*, 2002, **22**, 311–316.
3. Kondo, N., Ohji, T. and Fumihiro, W., Strengthening and toughening of silicon nitride by superplastic deformation. *J. Am. Ceram. Soc.*, 1998, **81**(3), 713–716.
4. Kondo, N., Suzuki, Y. and Ohji, T., Superplastic sinter-forging of silicon nitride with anisotropic microstructure formation. *J. Am. Ceram. Soc.*, 1999, **82**(4), 1067–1069.
5. Seabaugh, M. M., Kerscht, I. H. and Messing, G. L., Texture development by templated grain growth in liquid-phase-sintered alpha-alumina. *J. Am. Ceram. Soc.*, 1997, **80**(5), 1181–1188.
6. Imamura, H., Hirao, K., Brito, M. E., Toriyama, M. and Kanzaki, S., Further improvement in mechanical properties of highly anisotropic silicon nitride ceramics. *J. Am. Ceram. Soc.*, 2000, **83**(3), 495–500.
7. Uematsu, K., Ito, H., Zhang, Y. and Uchida, N., Novel characterization method for the processing ceramics by polarized light microscope with liquid immersion technique. *Ceram. Trans., Am. Ceram. Soc.*, 1995, **54**, 83–89.
8. Zhang, Y., Uchida, N. and Uematsu, K., Direct observation of non-uniform distribution of PVA binder in alumina green body. *J. Mater. Sci.*, 1995, **30**, 57–60.
9. Park, C. S., Kim, J. G. and Chun, J. S., Crystallographic Orientation and surface morphology of chemical vapor deposited Al_2O_3. *J. Electrochem. Soc.*, 1983, **130**, 1607–1611.
10. Yagi, I., Hagiwara, Y., Murakami, K. and Kaneko, S., Growth of highly oriented SnO_2 thin films on glass substrate from tetra-*n*-butyltin by the spray pyrolysis technique. *J. Mater. Res.*, 1993, **8**, 1481–1483.
11. Bae, S. I. and Baik, S., sintering and grain growth of ultra-pure alumina. *J. Mater. Sci.*, 1993, **28**, 4197–4204.
12. Bae, S. I. and Baik, S., Critical concentration of MgO for the prevention of aperpendicular grain growth in alumina. *J. Am. Ceram. Soc.*, 1994, **77**(10), 2499–2504.
13. Tartaj, J. and Messing, G. L., Effect of the addition of alpha-Fe2O3 on the microstructural development of boehmite-derived alumina. *J. Mater. Sci. Lett.*, 1997, **16**(2), 168–170.
14. Horn, D. S. and Messing, G. L., Anisotropic grain growth in TiO2-doped alumina. *Materials Science & Engineering A: Structural Materials: Properties, Microstructure & Processing*, 1995, **1**(2), 169–178.
15. Kebbede, A. and Carim, A. H., Influence of process variations on microstructure in doped sol-gel derived alpha-alumina. *Mater. Lett.*, 1998, **36**(1–4), 109–113.
16. Kebbede, A., Messing, G. L. and Carim, A. H., Grain boundaries in titania-doped alpha-alumina with anisotropic microstructure. *J. Am. Ceram. Soc.*, 1997, **80**(11), 2814–2820.
17. Sacks, M. D., Scheiffele, G. W. and Staab, G. A., Fabrication of textured silicon carbide via seeded anisotropic grain growth. *J. Am. Ceram. Soc.*, 1996, **79**(6), 1611–1616.
18. Kingery, W. D., Bowen, H. K. and Uhlmann, D. R., *Introduction to Ceramics*, (2nd edn.). John Wiley & Sons, New York, 1976.
19. Fullman, R. L., Measurement of particle size in opaque bodies. *Trans AIME*, 1953, **197**, 447–452.
20. Carisey, T., Levin, I. and Brandon, D. G., Microstructure and mechanical properties of textured Al_2O_3. *J. Eur. Ceram. Soc.*, 1995, **15**, 283–289.